Oxidation of Single Crystalline Ti_2AlN Thin Films between 300 and 900 ^oC: A Perspective from Surface Analysis

Zheng ZHANG,[†] Jianwei CHAI,[†] Hongmei JIN,[‡] Jisheng PAN,[†] Lai Mun WONG,[†] Suo Hon Lim,[†] Michael B. SULLIVAN,[‡] and Shi Jie WANG[†]***

[†] Institute of Materials Research and Engineering, A*STAR (Agency for Science, Technology and Research), #08-03, 2 Fusionopolis Way, Innovis, 138634, Singapore.

[‡] Institute of High Performance Computing, A*STAR (Agency for Science, Technology and Research), 1 Fusionopolis Way, Connexis, 138632, Singapore.

ABSTRACT

High temperature oxidation of 300 nm single crystalline Ti_2AlN MAX phase thin film deposited on MgO (111) substrate between 300 and 900 ºC has been investigated by X-ray diffraction (XRD), X-ray photoelectron spectroscopy (XPS), atomic force microscopy (AFM) and mass spectrometry. As shown by XRD, Ti_2AlN remained structurally stable up to 700 ºC, before it began to react with MgO substrate and ambient O_2 to form $MgTi_2O_5$ and $MgAl_2O_4$ at 900 ºC. However, as revealed by XPS, oxidation of Ti_2AlN occurred at room temperature from its surface by forming TiO_2, TiN_xO_y and Al_2O_3 with surface enrichment of Al. This initial oxidation continued up to 300 ºC, until Ti and Al in the surface layer (~7.1 nm thick) have been completely oxidized into TiO_2 and Al_2O_3 at 500 ºC, where Al in the subsurface preferentially diffused to the edges of the terraces and agglomerated into Al_2O_3 islands. At 700 ºC and above, surface of Ti_2AlN lost its characteristic hexagonal terrace morphology by transforming into round islands as a result of high temperature oxidation. Mass spectrometry revealed that N in Ti_2AlN was released from the MAX thin film as N_2 and N_2O.

I. Introduction

Ti_2AlN is a family member of the $M_{n+1}AX_n$ (n = 1-3) or MAX phase materials, where M corresponds to transition metals, A is a group 12-16 element and X is carbon and/or nitrogen. There are ~ 60 MAX phase materials which exhibit a common characteristic layered hexagonal structure (space group $P6_3/mmc$) constructed by vertically repeating two $M_{n+1}X_n$ layers intercalated by one layer of A in between.[1] Like other MAX phase materials, Ti_2AlN has attracted considerable interests recently due to its unique combination of both ceramic (high melting points and high temperature oxidation resistance) and metallic (good electrical and thermal conductivity, high ductility, easy machinability, etc) properties.[2] The distinctive combination of these properties stems from the co-existence of both strong covalent-ionic Ti-N bond and weak metallic Ti-Al bond inside Ti_2AlN.[1-3]

Bulk polycrystalline Ti_2AlN was first fabricated through hot isostatic pressing of Ti and AlN powders at 1600 ^oC in 1997.[4] From 2005 onwards, single crystalline[3,5-9] and polycrystalline Ti_2AlN thin films[10-11] have been synthesized using one-step sputtering technique. Alternatively, Ti_2AlN phase can be produced by a post-deposition vacuum-annealing of Ti-Al-N thin films [12-13] or multilayered structures (i.e., TiN/TiAl(N),[14] (Ti+Al)/AlN,[15] etc). The capability to deposit Ti_2AlN MAX phase thin films on different substrates including MgO,[3,5-9,11] Al_2O_3,[6,10,12] Si,[10,13-14] steel[13] and SiC[15] has enabled the exploration of its exceptional properties in a variety of applications. One of them is as a protective coating in high temperature environments such as automobile/aircraft engine components, heating elements, heat exchangers, gas burner nozzles, etc. Two critical aspects that need be considered for high temperature application are high-temperature phase stability and oxidation resistance. The studies on phase stability aspect generally agree that Ti_2AlN does not melt congruently in vacuum but decomposes via

preferential loss of Al through desorption from Ti_2AlN.[6,16-20] It has been agreed that thin film samples usually decompose at lower temperatures compared to bulk samples. A lower base pressure would further decrease the decomposition temperature.

Pertaining to the other aspect of oxidation resistance, Barsoum *et al* proposed a generalized model describing oxidation of bulk $Ti_{n+1}AlX_n$ in the 800 - 1100 ^oC temperature range, where oxidation occurs via inward diffusion of oxygen and outward diffusion of Al^{3+} and Ti^{4+} ions. The oxidation products are Al_2O_3 and Al-dissolved TiO_2, i.e., $(Ti_{1-x}Al_y)O_{2-y/2}$, where $y < 0.05$.[21] This oxidation model has been verified experimentally on Ti_2AlC, $Ti_2AlC_{0.5}N_{0.5}$, $Ti_4AlN_{2.9}$ and Ti_3AlC_2 (but not on Ti_2AlN) by the same author,[22] who recently commented that the oxidation kinetics of Ti_2AlC and Ti_3AlC_2 are better described by cubic kinetics (rather than parabolic kinetics), and the rate-limiting step is the diffusion of oxygen and/or aluminum ions down the Al_2O_3 scale grain boundaries.[23] A separate study by Bai *et al* on the oxidation of bulk Ti_2AlN observed formation of anatase TiO_2, rutile TiO_2 and α-Al_2O_3 after one hour oxidation at temperature lower than 1200 ^oC, while a more complex structure containing Al_2TiO_5, rutile TiO_2 and continuous void layers was formed after one hour oxidation at temperature higher than 1200 ^oC.[24] In contrast to bulk Ti_2AlN, oxidation of 5 ~ 6 μm polycrystalline Ti_2AlN thin films did not result in formation of TiO_2 significantly.[10,25-26] Instead, Kim *et al* observed that Al preferentially diffused to surface and formed a θ-Al_2O_3 layer upon oxidation at 800 ^oC, which transformed into α-Al_2O_3 scale at 900 ^oC.[10,25-26] The resultant continuous Al_2O_3 oxide scale protected the Ti_2AlN and the substrate below effectively from further oxidation. While these works have mainly focused on the oxidation products of Ti and Al so far, the oxidation product of nitrogen inside Ti_2AlN has been far less investigated. Barsoum *et al* proposed in his theoretical model that nitrogen leaves the Ti_2AlN as NO or NO_2 after oxidation,[21] while Bai *et al* presumed that

nitrogen was oxidized into gaseous NO_x.[24] Nevertheless, no experimental evidence was able to verify these assumptions. It is worth noting that nitrogen has been detected to leave TiN as NO and N_2 after oxidation by mass spectrometry.[27] Hence the oxidation products for the nitrogen in Ti_2AlN could be rather complex.

We have deposited single crystalline Ti_2AlN thin films on MgO (111) substrates by sputtering a Ti_2Al alloy target in a mixed N_2/Ar plasma at 750 ºC.[9] The single crystalline thin film would offer the opportunity to probe the intrinsic material properties of Ti_2AlN, because unlike amorphous and polycrystalline phases, single crystalline phase has a periodic microscopic structure extending in all directions and has less influence from grain boundaries and grain sizes. Hence, we have investigated the thermal stability of 400 nm single crystalline Ti_2AlN thin film in ultra-high-vacuum (UHV) and found that Ti_2AlN is stable up to 600 ºC while Al is preferentially lost from the surface through desorption at 700 ºC and above.[20] The single crystalline Ti_2AlN with terrace morphology transforms into polycrystalline TiN_{1-x} and $TiN_{0.75-y}$ phases with voids on the surface as well as reduced film thickness at 900 ºC.

To shed more light on the oxidation of Ti_2AlN, especially in thin-film form,[10,21-22,24-26] we take advantage of the availability of single crystalline Ti_2AlN thin film and oxidize the single crystalline Ti_2AlN thin film in a furnace at different temperatures. We subsequently characterized the oxidized thin film using X-ray diffraction (XRD), X-ray photoelectron spectroscopy (XPS) and atomic force microscopy (AFM) with emphasis on the development of surface chemistry and morphology with respect to oxidation temperature. We will show that the 300 nm single crystalline Ti_2AlN MAX phase thin film started to be oxidized at room temperature by forming TiO_2, TiN_xO_y and Al_2O_3 with surface enrichment of Al in form of Al_2O_3. Ti and Al in the surface layer (~7.1 nm thick) were completely oxidized into TiO_2 and Al_2O_3 at 500 ºC and above, while

the whole 300 nm film remained structurally stable up to 700 ^{o}C, before it reacted with MgO substrate and ambient O_2 to form $MgTi_2O_5$ and $MgAl_2O_4$ at 900 ^{o}C. A separate mass spectrometry measurement substantiated the XPS observation that N in Ti_2AlN was released from the MAX thin film as N_2 and N_2O.

II. Experimental methods

300 nm single crystalline Ti_2AlN (002) thin film was deposited on MgO (111) substrate at 750 ^{o}C after sputtering a 3 inch Ti_2Al alloy target (99.99% purity) at a power of 90 W in a mixture of Ar (3.2×10^{-3} mbar) and N_2 (6.0×10^{-5} mbar) plasma for 1 hour.[9] After deposition, the Ti_2AlN thin film was annealed in a Carbolite 1200 box furnace three hours each at 300, 500, 700 and 900 ^{o}C in ambient environment. After cooling down at each temperature, the Ti_2AlN thin film was then taken out of the furnace and its crystalline structure was investigated using Bruker general area detector diffraction system (GADDS) XRD operated at a voltage of 40 kV and a current of 40 mA (Cu Kα X-ray, λ=1.54Å). The surface composition and surface morphology of the sample were subjected to analysis by VG ESCALAB 220i-XL XPS and Bruker Dimension ICON AFM, respectively. A separate Ti_2AlN single crystalline sample was loaded into the same growth chamber which has been installed with a Stanford Research System closed ion source gas analyzer (SRS CIS 200 mass spectrometer) in the nearest port adjacent to the manipulator. The sample was heated up to 400, 500 and 600 ^{o}C using resistive heating and monitored by a pyrometer. At each temperature, after the base pressure was recovered back to ~3.0×10^{-6} mbar, the pure O_2 gas (99.995%) was rapidly introduced into the chamber via a leak valve to a pressure of 5.5×10^{-5} mbar, which was maintained for 3 mins before the leak valve was quickly turned off

and allowed the base pressure to recover. Subsequently, the temperature was raised up again. Partial pressures of the five different species including N_2, NO, O_2, N_2O and NO_2 with *m/e* of 28, 30, 32, 44 and 46, respectively, were continuously monitored by the mass spectrometer at each temperature.

III. Results and Discussion

The XRD patterns of the 300 nm Ti_2AlN thin film after oxidation annealing between 300 and 700 ºC show that only Ti_2AlN (0002) and (0006) peaks were detected, indicating that the crystalline structure of the Ti_2AlN thin film remained stable up to 700 ºC (Fig. 1). Though different in crystallinity, the 5 - 6 μm polycrystalline Ti_2AlN thin film was also reported to remain stable by XRD up to 700 ºC after oxidation annealing.[26] The good oxidation resistance of single crystalline Ti_2AlN thin film does reflect the excellent oxidation resistance of bulk Ti_2AlN[24] as well as other bulk MAX phase materials (Ti_2AlC,[28] Ti_3AlC_2,[29] etc). At 900 ºC, this single crystalline film was oxidized into a mixture of rutile TiO_2, $MgTi_2O_5$ and $MgAl_2O_4$. The presence of these three phases was further confirmed through full pattern Rietveld phase analysis of the XRD pattern, which is shown in Fig. S1 of the Supporting Information. The latter two spinel phases are most likely due to the reaction between oxidation product of Ti_2AlN (TiO_2 & Al_2O_3) and MgO substrate at 900 ºC. This $MgAl_2O_4$ and other spinel phase like Mg_2TiO_4 have similarly been detected at the interface between Ti_2AlN and MgO substrate by Rutherford backscattering spectroscopy (RBS)[6] and time-of-flight secondary-ion-mas-spectroscopy (TOF-SIMS)[20] when the single crystalline Ti_2AlN thin films grown on MgO (111) substrates were annealed in a UHV condition. The reaction between Al_2O_3 and MgO to form $MgAl_2O_4$ spinel phase at 900 ºC likely explains why Al_2O_3 phase was not detected by XRD in our work.

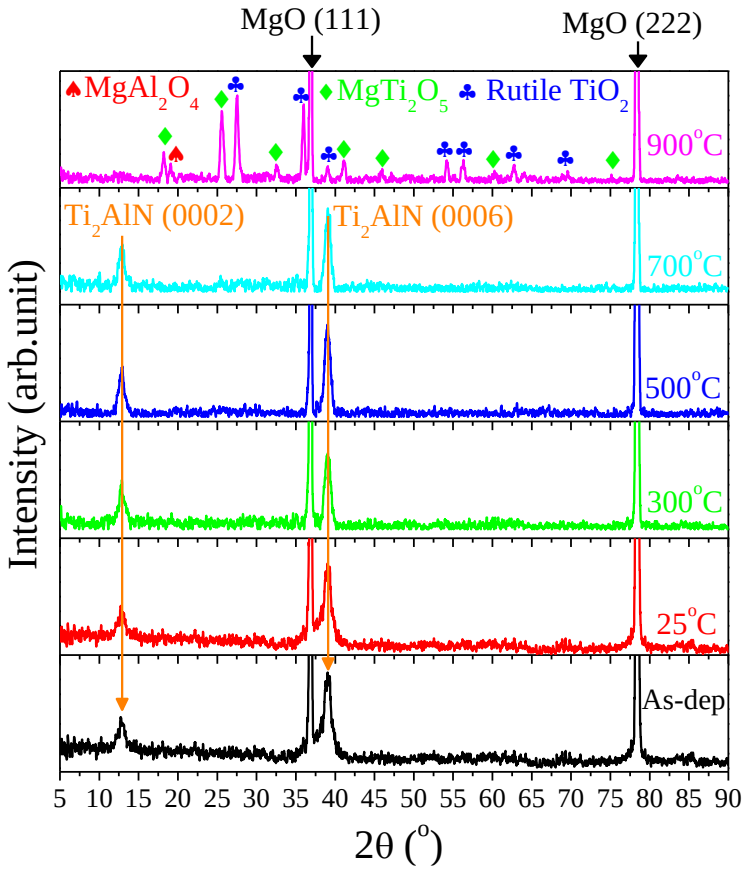

Fig.1 The X-ray diffraction patterns of the as-deposited 300 nm Ti_2AlN single crystalline thin film (black), after oxidation at room temperature (25 ºC) in ambient air (red) and subsequently oxidized 3 hours at 300 (green), 500 (blue), 700 (cyan) and 900 ºC (pink) inside a furnace.

In order to understand the chemical states of Ti and Al after oxidation, we examined the surface of Ti_2AlN thin film by XPS after oxidation at every temperature. The XPS spectra are scaled to have same height and are stacked in Fig. 2 for easy comparison. Ti $2p_{3/2}$, Al $2p_{3/2}$ and N 1s showed a single chemical state at 454.7, 72.3 and 397.4 eV, respectively, right after *in-situ* deposition. The difference in spin-split between $2p_{3/2}$ and $2p_{1/2}$ (Δ) are 6.0 and 0.4 for Ti 2p and Al 2p, respectively. As discussed previously, binding energy (BE) of Al $2p_{3/2}$ at 72.3 eV together with characteristic Ti *3d* – Al *3p* hybridization peak between 0 and 4 eV in valence band (Fig.

2(d)) can be served as a fingerprint to identify formation of Ti_2AlN MAX phase material.[9] After oxidation in air, two new pairs of doublets appeared in the Ti 2p spectrum: one broad peak (Ti $2p_{3/2}$: 457.9, Ti $2p_{1/2}$: 463.5 eV) and the other sharp peak (Ti $2p_{3/2}$: 459.0 eV, Ti $2p_{1/2}$: 464.8 eV, red spectra in Fig. 2(a)). Two additional peaks also appeared in N 1s spectrum: one sharp peak at 396.4 eV and one broad peak at 400.2 eV (Fig. 2(c)). By referring to the oxidation process of TiN,[30-31] we attribute Ti $2p_{3/2}$ at 456.9 eV with Δ of 5.6 and N 1s at 396.4 eV to TiN_xO_y, Ti $2p_{3/2}$ at 459.0 eV with Δ of 5.8 eV to TiO_2 and N 1s at 400.2 eV to N-O bond, respectively. For Al 2p spectrum, an extra doublet peaks at 74.5 eV (Al $2p_{3/2}$) and 74.9 eV (Al $2p_{1/2}$) appeared which can be attributed to Al_2O_3.[32] The intensities of characteristic Ti *3d* – Al *3p* hybridization peak between 0 and 4 eV, Ti *3d* – N *2p* hybridization peak between 4 and 8 eV in the valence band (VB) and N 2s at 16.9 eV decreased (Fig. 2(d)) due to the reduction of the valence electrons from Ti, Al and N following their oxidation at room temperature. At the same time, intensity of O 2s peak around 22.5 eV in VB increased substantially. In O 1s spectrum (Fig. 2(e)), there were three components at 530.5, 532.8 and 534.0 eV, corresponding to oxides (TiO_2 and Al_2O_3), epoxy/alkoxy/ether-like species (O-C)/oxynitride (O-N) and adsorbed water species (H_2O), respectively.

After oxidizing three hours at 300 ^oC, the oxidation products on the surface still remained the same. However, the intensities of the oxides (green spectra in Fig. 2(a-c)), i.e., TiO_2 (459.0 eV in Ti 2p), Al_2O_3 (74.2 eV in Al 2p), TiN_xO_y (396.4 eV in N 1s), have increased significantly compared to their counterparts at room temperature (red spectra in Fig. 2(a-c)). The Ti *3d* – Al *3p* hybridization between 0 and 4 eV, Ti *3d* – N *2p* hybridization between 4 and 8 eV and N 2s at 16.9 eV in VB continued to decrease due to declining valence electron densities caused by further oxidation of all three elements in Ti_2AlN (green spectrum in Fig. 2(d)), while the O-C/O-

N peak at 532.2 eV in Fig. 2(e) decreased due to desorption of the gaseous absorbent at elevated temperature. The shift of O-C/O-N component from 532.8 eV after oxidation at room temperature to 532.2 eV after oxidation at 300 ºC is likely attributed to higher O-N ratio in this component due to heavier oxidation of Ti_2AlN at 300 ºC and more O-N bonding formation.

After oxidizing three hours at 500 ºC, there was only one component in Ti $2p_{3/2}$ (459.0 eV) and Al $2p_{3/2}$ (74.2 eV) peaks, which indicates Ti and Al within probing depth of XPS were completely oxidized into their highest oxidation states, TiO_2 and Al_2O_3, respectively. For N 1s, the peak at 397.4 eV corresponding to Ti_2AlN disappeared completely. Probing depth of XPS dominantly covers a layer with thickness equal to three times of photoelectron's inelastic mean free path (λ). λ is calculated to be 2.36 and 2.56 nm for Ti $2p_{3/2}$ and Al $2p_{3/2}$ photoelectrons,[33] respectively. Hence, the XPS results imply that the top surface layer with a thickness of ~7.1 nm ($3\lambda_{Ti}$) was completely oxidized at 500 ºC. It is worth noting that there were two peaks in N 1s spectrum: one at 396.4 eV and the other at 403.3 eV. The one at 396.4 eV has been detected at lower temperature too and was assigned to TiN_xO_y. The other at 403.3 eV was a new component and is likely to be attributed to N_2, based on the oxidation product of TiN.[30-31] XPS result thus indicates oxidation product of N could be a mixture of NO/N_2O and N_2, which will be further discussed in a separate mass spectrometry experiment later. The Ti *3d* – Al *3p* and Ti *3d* – N *2p* hybridization in VB have reduced to their lowest intensity and remained roughly unchanged up to 900 ºC, as both Ti and Al at the surface were completely oxidized and bonded with oxygen instead. In O 1s spectrum, the H_2O component at 534.0 eV was completely vanished and the hydrocarbon (C-O) component at 532.8 eV further decreased, both due to adsorbents' desorption at high temperature.

Further oxidation at 700 ºC for three hours has led to complete loss of nitrogen (cyan

curve in Fig. 2(c)), which has been similarly observed earlier.[26] Oxidation at 900 °C resulted in a shift of Al $2p_{3/2}$ from 74.2 to 74.6 eV. In addition, significant Mg 1s signal (pink curve in Fig. 2(f)) and the additional peak at 530 eV in O 1s spectrum were detected (Fig. 2(e)). Both these two peaks as well as Al $2p_{3/2}$ at 74.6 eV[34] are believed due to the formation of spinel phases ($MgTi_2O_5$ and $MgAl_2O_4$), which has been detected by XRD after reaction of TiO_2, Al_2O_3 and MgO substrates at 900 °C (Fig. 1). Different from Bai *et al* who detected Al_2TiO_5 by XRD after oxidizing bulk Ti_2AlN for one hour at higher than 1200 °C,[24] we did not detect Al_2TiO_5 formation in this present study. This is not unexpected as according to Al-O-Ti phase diagram, TiO_2 and Al_2O_3 are mutually insoluble and are calculated not to form ternary compounds (i.e., Al_2TiO_5) below 1300 °C under an oxygen partial pressure of 0.21 bar (ambient condition).[35] The highest oxidation temperature is 900 °C in our work, which is far below the threshold temperature (1300 °C) and thus does not result in the formation of Al_2TiO_5.

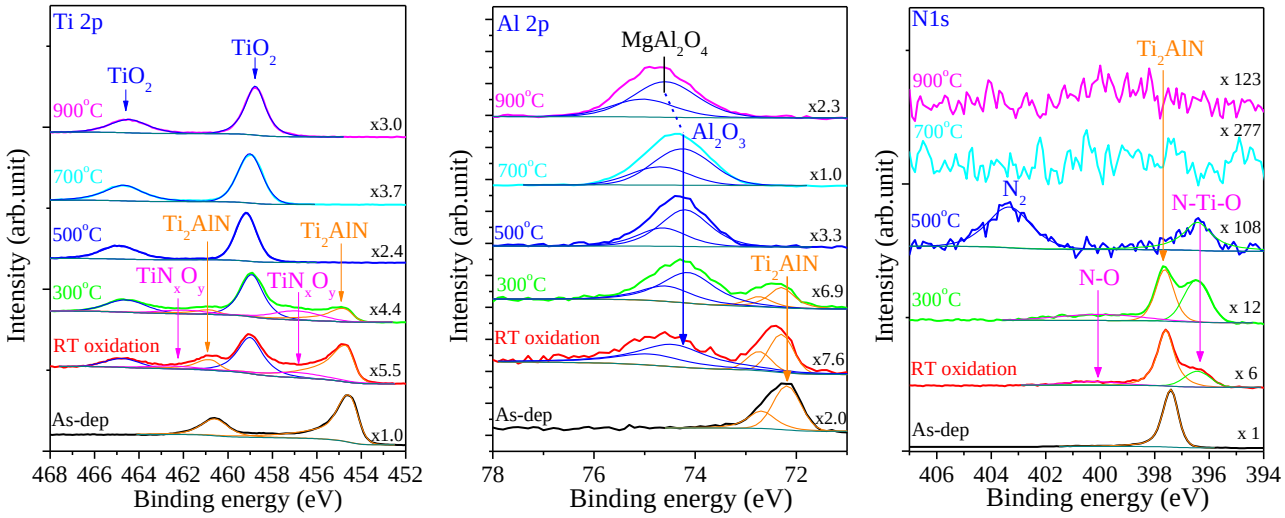

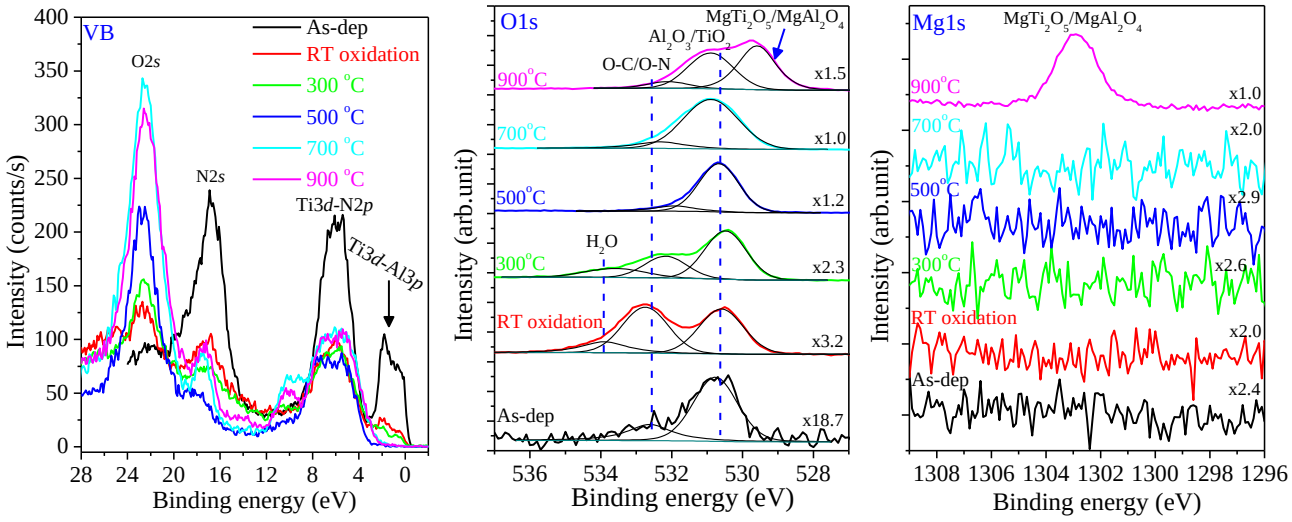

(d) (e) (f)

Fig. 2 High resolution XPS spectra of (a) Ti 2p, (b) Al 2p, (c) N 1s, (d) valence band (VB), (e) O 1s and (f) Mg 1s from as-deposited Ti_2AlN single crystalline thin film and after oxidization at room temperature as well as in furnace at 300, 500, 700 and 900 ºC for 3 hours. The spectra in each figure (except VB) are normalized to have the same maximum peak heights with the scaling factor indicated near the right axis of each spectrum for easy comparison.

The composition of Ti, Al, N, O and Mg as a function of oxidation temperature is plotted in Fig. 3 based on the peak areas before scaling in Fig. 2, in order to understand the relative movement of these elements at different oxidation temperatures. There was a consistent increase in percentage of O from 52.9 % at room temperature to 63.5 % at 500 ºC due to continual oxidation of Ti and Al and hence persistent uptake of oxygen from ambient air (Fig. 3(a)). Percentage of N continued to decrease from 40.0 % after deposition to 0 % at 700 ºC and above due to desorption of N as gaseous species. Percentage of Al remained stable around ~9 - 10 % up to 300 ºC and increased to 29.1 % at 700 ºC before it decreased to 18.2 % at 900 ºC. On the other hand, percentage of Ti remained stable between 25 and 500 ºC at around 22 % before it decreased to 9.1 % at 700 ºC and 12.9 % at 900 ºC. The relative ratio of Ti% / Al% as a function of oxidation temperature is plotted in Fig. 3(b). It can be seen that Ti % / Al % decreased as soon

as the sample was oxidized at room temperature and the ratio continued decreasing till 700 ºC. This trend indicates that there is an apparent Al preferential surface segregation during oxidation of Ti_2AlN from room temperature to 700 ºC.

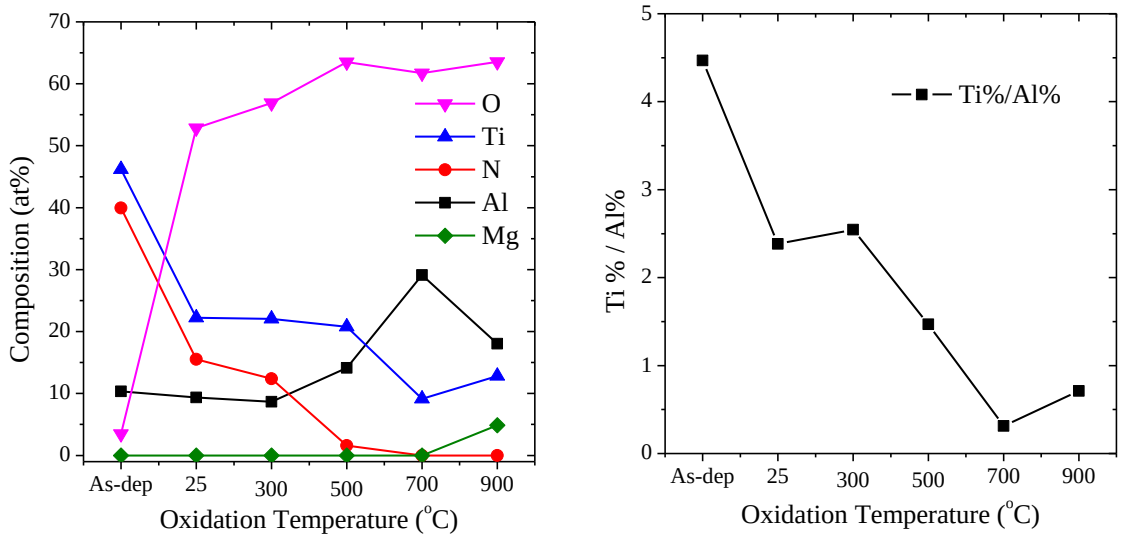

(a) (b)

Fig. 3 (a) The composition development of the Ti_2AlN single crystalline thin film after oxidizing at 25 ºC and annealing 3 hours in furnace at 300, 500, 700 and 900 ºC. It is calculated based on the corresponding peak areas from in Fig. 2 before normalization. (b) The plot of Ti% / Al% ratio as a function of oxidizing temperature derived from (a).

The depth profiling of Ti, Al, N and O after oxidation at room temperature and 500 ºC are shown in Fig. 4 to display the depth distribution of elements during oxidation. The sputtering rate based on Ta_2O_5 is calibrated to be 2.7 nm/min. There was a slight enrichment of Al % at the surface upon oxidation at room temperature, and the composition of Ti, Al, N and O % recovered to the bulk value after sputtering for two minutes (Fig. 4(a & b)). Upon oxidation at 500 ºC for 3 hours, there was a clear surface enrichment of Al%, O% and Ti% (Fig. 4(c & d)), which can be attributed to outward diffusion of Al and Ti together with inward diffusion of oxygen. Meanwhile, there was a loss of N from surface (Fig. 4(d)), which agreed with the decreasing

trend of N% with oxidation temperature (Fig. 3(a)) and N% was only reached the bulk value after sputtering for ten minutes.

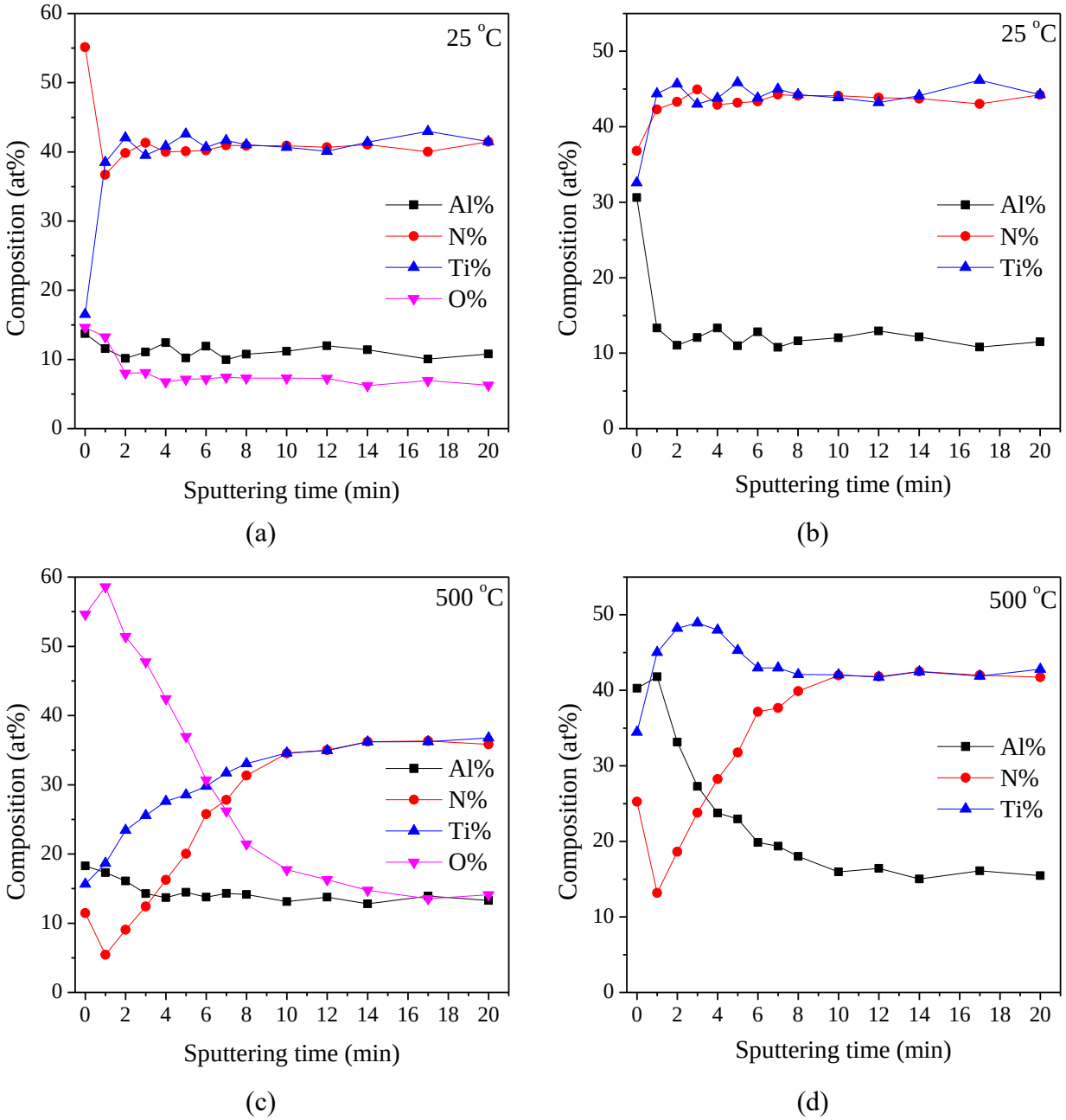

Fig. 4 XPS depth profiling of the atomic composition of 300 nm Ti_2AlN thin film after oxidation at (a & b) room temperature and (c & d) 500 ºC for 3 hours. a & c calculate the compositions including Ti, Al, N and O, while b & d only consider the composition including Ti, Al and N.

The surface enrichment of Al during oxidation will likely cause a change in surface

morphology. Hence, the surfaces of Ti_2AlN after oxidation at each temperature were examined under AFM and are shown in Fig. 5. After oxidizing at room temperature, surface of Ti_2AlN still displayed the characteristic hexagonal layered terrace morphology with a dominant step height of 1.42 ± 0.15 nm (green line, Fig. 5(a)). Terraces with step height of 0.71 ± 0.06 nm can be also found occasionally (purple line, Fig. 5(a)). These two values correspond to the heights of one unit cell and half-unit cell of Ti_2AlN, respectively, characteristic of the well-known step-flow growth mode of MAX phases. Such terrace morphology has similarly been observed on the surfaces of Ti_3SiC_2[36-37] and Ti_3GeC_2[38] thin films.

The oxidation of Ti_2AlN at surface into TiO_2, TiN_xO_y and Al_2O_3 at room temperature detected by XPS (Fig. 2) seems having little influence on the surface morphology. Our earlier DFT calculation shows that of Ti_2AlN is thermodynamically favorable to have Al-terminated surface followed by Ti_1-terminated (Ti_1 atom bonds directly with Al atom while Ti_2 atom bonds directly with N atom) surface.[39] Meanwhile, percentage of Al is only 12.0 % in the bulk of thin film (Fig. 4(b)), which indicates presence of significant amount of Al vacancies. Hence, oxidation at the room temperature could occur via adsorption of O_2/H_2O onto the Al-terminated and/or Ti-terminated surfaces of Ti_2AlN, which forms O-Al and/or O-Ti-Al bonds. Oxidation could also occur via diffusion of O_2 from the top Ti layer into the Al layer right below, where Al vacancies are present and O-Al / O-Ti bonds could form. Both oxidation pathways do not cause severe distortion of the Ti_2AlN crystalline structure and hence its surface morphology. Although the percentage of Al is below the stoichiometric value of 25 %, our recent DFT calculation showed that Ti_2AlN is capable of accommodating Al vacancies in the supercell down to a sub-stoichiometric $Ti_2Al_{0.75}N$ while maintaining the MAX phase structure.[40]

Oxidation at 300 ^oC does not incur dramatic change in the hexagonal layered terrace

morphology too (Fig. 5(b)). However, the terraces at 300 ºC appeared to be much rougher compared to the ones at room temperature in the 2 × 2 μm^2 image, which is reflected as an increase in root-mean-square (RMS) roughness from 1.35 nm at room temperature to 2.72 nm at 300 ºC.

After oxidizing at 500 ºC where both Ti and Al at the surface layer were completely oxidized into TiO_2 and Al_2O_3 (Fig. 2(a&b)) while percentage of Al started to increase clearly (Fig. 3(a)), small domes with an average diameter of 24.01 ± 5.68 nm and height of 1.98 ± 0.90 nm were observed sitting on top of the surfaces. From the high resolution 2 × 2 μm^2 AFM image, it can be seen that these domes typically lined up along the edges of the terraces when terraces are still preserved (area marked by the circle), or agglomerate without stacking on top of each other at the surface where terrace morphology is not discernible (area marked by the rectangle).

Similar small round features with a diameter of tens of nanometers have been observed by SEM when 1 μm Ti_2AlC thin film was oxidized at 500 ºC in ambient air for 5 minutes.[41] Frodelius *et al* attributed the small granular/circular islands to amorphous Al_2O_3.[41] Our recent density function theory (DFT) calculation shows that Al atoms requires to overcome a self-diffusion barrier of only 0.7 ~ 0.8 eV when diffusing horizontally in Ti_2AlN, compared to an energy barrier of more than 1.65 eV when diffusing vertically.[40] It is also much lower than the 2.7 and 2.9 eV energy barriers for Ti and N atoms to diffuse along (0001) plane, respectively.[40] Meanwhile, the Ti-Al bonding is much weaker than the Ti-N bond.[9] Hence, for Al-terminated surfaces, Al atoms were likely to bond directly with oxygen atoms, agglomerate as Al_2O_3 domes on the surface and lose its terrace morphology (such as the rectangular area). For Ti_1-terminated surfaces, Al atoms at the subsurface (i.e, right below the surface Ti_1 layer) were likely to gain sufficient kinetic energy at 500 ºC to diffuse horizontally to the edge of its layer, meet oxygen

from ambience, react with it to form Al_2O_3 and agglomerate along the edge of the terrace (such as the circle area). Therefore, similar to the formation of Al_2O_3 round features after oxidation of Ti_2AlC thin film,[41] the round islands appeared after oxidation of Ti_2AlN thin film at 500 ºC are also likely to be Al_2O_3, which correlates well the enrichment of Al over Ti observed at 500 ºC observed by XPS (Fig. 3(b)). Such Al surface segregation could start at as low as room temperature so that the Ti%/Al% significantly decreased after room temperature oxidation (Fig. 3(b)). Nevertheless, the Al_2O_3 did not agglomerate as heavily as it did at 500 ºC due to low mobility at room temperature, and hence formation of room islands was not observed by AFM below 500 ºC. The terrace morphology was still retained at 500 ºC, which agrees well with XRD results that the Ti_2AlN MAX phase was still present at 500 ºC (Fig. 1).

The AFM image (Fig. 5(c, ii)) shows clearly that the coverage of Al_2O_3 in this work is not high enough to form a continuous protective layer over the entire surface, thus part of the terraces was still exposed to air and both Ti and N were also oxidized. The percentage of Al is 20.32 % in the 5 - 6 μm polycrystalline Ti_2AlN Kim *et al* deposited,[10,26] which is almost twice higher than ours (12.0 %). They observed formation of a dense and continuous α-Al_2O_3 scale with equiaxed α-Al_2O_3 crystallites by SEM after oxidation of the Ti_2AlN thin film for 20 hours at 900 ºC.[26] It is likely that the concentration of Al in their Ti_2AlN films is sufficiently high to produce a continuous α-Al_2O_3 scale, which prevents Ti and N in Ti_2AlN from severe oxidation and explain why they only observed an α-Al_2O_3-rich scale formation after oxidation. The Al_2O_3 detected after oxidation from room temperature to 300 ºC in present work is likely to be amorphous. The small Al_2O_3 circular islands formed after oxidation at 500 ºC had a height of only 1.98 ± 0.90 nm. They are likely to be α-Al_2O_3 phase as they also possess the equiaxed shape, similar to the equiaxed α-Al_2O_3 crystallites Kim *et al* detected at 900 ºC.[26] However, their

crystallinity is unlikely to be convincingly determined here even with grazing-incidence XRD due to incomplete coverage and small thickness.

At 700 ºC, the surface has completely lost its characteristic hexagonal layered terrace morphology by changing into a morphology comprised of circular islands with an average diameter of 36.68 ± 7.01 nm and height of 8.43 ± 2.69 nm, although XRD shows the bulk of the thin film still retained the Ti_2AlN structure (Fig. 1). At 900 ºC when the film was oxidized into mixture of rutile TiO_2, $MgTi_2O_5$ and $MgAl_2O_4$ (Fig. 1), the small circular islands observed at 700 ºC agglomerated and developed into much bigger circular islands with average diameter of 289.10 ± 44.64 nm and a height of 48.62 ± 14.60 nm. Apparently the oxide islands have grown in diameter and height with temperature from 500 to 900 ºC, which results in a linear increase in RMS roughness of the 2 × 2 μm^2 AFM images from 2.87 nm (500 ºC) to 14.13 nm (700 ºC) to 34.81 nm (900 ºC).

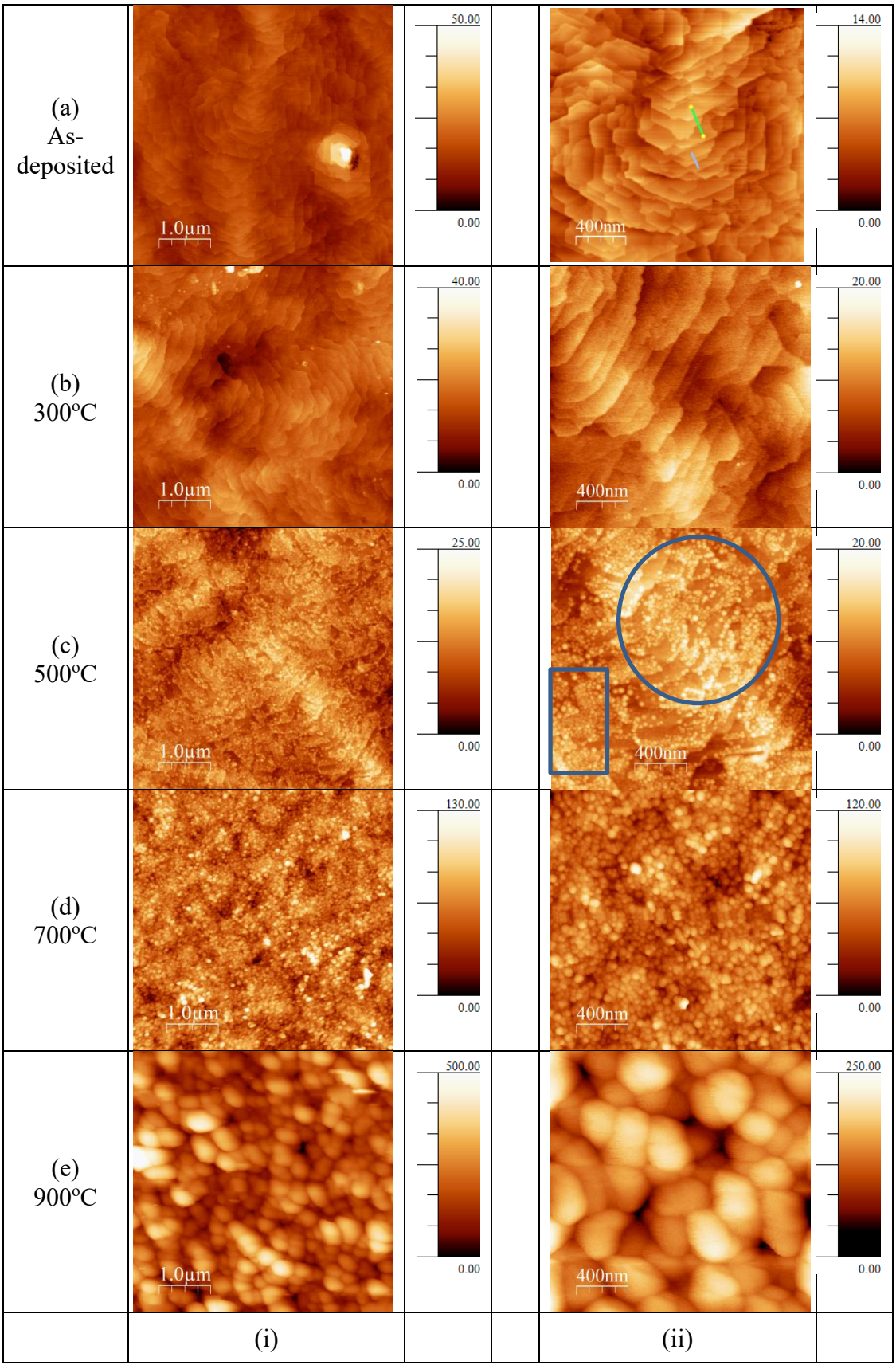
(a) As-deposited
(b) 300°C
(c) 500°C
(d) 700°C
(e) 900°C
1.0µm
400nm
50.00
0.00
14.00
40.00
20.00
25.00
130.00
120.00
500.00
250.00
(i)
(ii)

Fig. 5 Column (i) 5 × 5 μm^2 (left panel) and (ii) 2 × 2 μm^2 (right panel): AFM images of (a) as-deposited Ti_2AlN thin films and after oxidation for 3 hours at (b) 300, (b) 500, (c) 700 and (d) 900 ^oC

The oxidation products of N in Ti_2AlN and other nitride-based MAX phase materials are still ambiguous in the literature. Several possible products including NO, NO_2 or N_2 have been proposed but none of them has been verified experimentally. XPS detected formation of N-O species between room temperature to 300 ^oC and N_2 at 500 ^oC. Different gaseous species have different surface adsorption coefficients and it is not ideal to use *ex-situ* XPS to examine the evolvement adsorbed on the surface after oxidation in furnace. To compliment XPS observation and to determine the real time evolvement products, we oxidized a separate Ti_2AlN single crystalline thin film sample under high vacuum environment in the growth chamber using pure O_2 gas and monitored its evolvement at 400, 500, and 600 using mass spectrometry, before the Ti_2AlN decomposed at 700 ^oC in ultra-high-vacuum condition[20]. The results at these three temperatures were nearly identical, hence only the pressure vs time plot at 500 ^oC was shown in Fig. 6 as an example. Before the Ti_2AlN sample was introduced, pure O_2 was introduced into the chamber until the base pressure increased from 3.0×10^{-6} mbar to 5.5×10^{-5} mbar. The partial pressure of N_2, NO, N_2O and NO_2 with *m/e* of 28, 30, 44 and 46, respectively, were continuously monitored (Fig. 6 (a)). There was no obvious increase in the partial pressure of these four species (Fig. 6 (a)), indicating that the O_2 gaslines are clean after purging since presence of N_2 and CO_2 as residual air in the gaslines will lead to a rise in partial pressure of N_2 and N_2O (*m/e* for both N_2O and CO_2 are 44). After Ti_2AlN thin film was transferred into the chamber and heated up to 500 ^oC, the partial pressure of N_2 and N_2O increased almost instantaneously following the introduction of O_2, while the partial pressure of NO and NO_2 did not show discernible changes

(Fig. 6(b)). As soon as the O_2 leak valve was closed, the pressure of N_2 and N_2O were restored back to the base level. While it is not surprising to detect N_2O as an oxidation product of nitrogen, it is unexpected to detect N_2 by both XPS (Fig. 2(c)) and mass spectrometry (Fig. 6(b)). Nevertheless, N_2 was also detected by XPS after both electrochemical and thermal oxidation of TiN and ZrN thin films.[42] It is believed to be partially trapped in the uppermost part of the oxide layers formed. Hence, N_2 can similarly be trapped into the top oxide layer after oxidation of Ti_2AlN and can be detected by XPS at 500 °C, before it is completely desorbed at higher oxidation temperature. It can be inferred that N in Ti_2AlN was oxidized into N_2O and N_2 and the oxidation pathway can be expressed as

$$8Ti_2AlN(s) + 23O_2(g) \xrightarrow{\Delta} 16TiO_2(s) + 4Al_2O_3(s) + 2N_2(g) + 2N_2O(g)$$

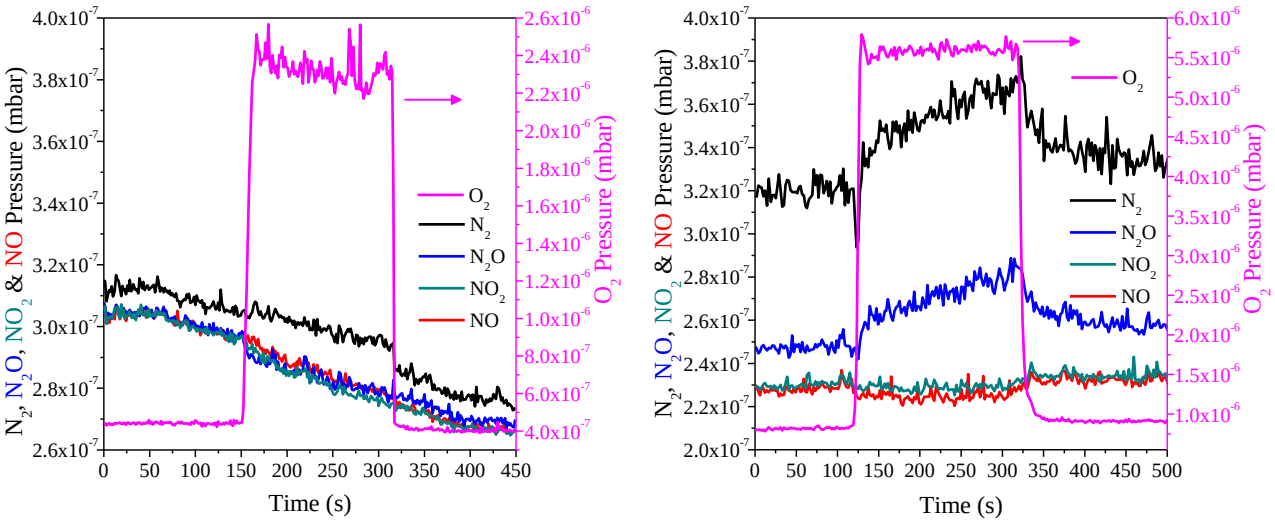

Fig. 6 Partial pressures of N_2, NO, O_2, N_2O and NO_2 monitored by the SRS CIS 200 mass spectrometer (a) without and (b) with exposing a 300 nm single crystalline Ti_2AlN thin film sample to pure O_2 gas via leak valve at 500 °C.

Al has a higher vapor pressure than Ti, and hence Al tends to evaporate easier than Ti. When Al-containing MAX phases (i.e., Ti_2AlN,[17-18,20] Ti_4AlN_3[18] and Ti_2AlC[43]) were heated up in

vacuum environments, preferential desorption of Al has thus accounted for the decomposition of these Al-containing MAX phase materials in high vacuum condition. In this present case of oxidation (heating up in air), another factor, heat of formation ($\Delta_f H^o$) of oxides, plays a more decisive role. $\Delta_f H^o$ of α-Al_2O_3 (-1675.7 kJ/mol) at 298.15 K and 1 atm is significantly lower than that of rutile-TiO_2 (-944.0 kJ/mol),[44] thus it is energetically favorable for Al over Ti to be oxidized in Ti_2AlN. In addition, the Ti-Al bonding is calculated to be weaker than the Ti-N bond.[9] Indeed, our XPS results indicate a preferential surface enrichment of Al over Ti during oxidation from room temperature to 700 ºC (Fig. 3(b)), which shows that Al is also kinetically favorable to be oxidized over Ti at this temperature range and agrees with the theoretical prediction that oxidation of bulk $Ti_{n+1}AlX_n$ in the 800 - 1100 ºC temperature range occurs via outward diffusion of Al^{3+} ions[21] as well as other experimental observation.[10,22] Such surface enrichment of Al over Ti during oxidation depends on $\Delta_f H^o$ of their oxides but not on the crystallinity of Ti_2AlN thin film, therefore it has been similarly reported during initial oxidation of polycrystalline Ti_2AlN thin film,[10,26] bulk Ti_2AlN sample[24] and even a series of $Ti_{1-x}Al_xN$ thin films with various Al%[45].

The percentage of Al in $Ti_{1-x}Al_xN$ film is critical to the oxidation resistance of the $Ti_{1-x}Al_xN$ coatings by affecting its oxidation activation energy and changing oxide layer thickness.[45] Similarly, it also influences the oxidation resistance of Ti_2AlN coating. The low Al concentration in Ti_2AlN thin film in our work (12.0 % Al) with a small thickness (300 nm) do not lead to formation of continuous Al_2O_3 scale, which is otherwise observed in Kim *et al*'s 5 - 6 μm polycrystalline Ti_2AlN thin film with 20% Al.[25] Thickness of the coating also affects the oxidation resistance. While the center 5 - 6 μm polycrystalline Ti_2AlN thin film exhibit good oxidation resistance at 900 ºC, a 2 - 3 μm polycrystalline Ti_2AlN thin film on the edge of the

same TiAl substrate has been fully oxidized at 900 ºC.[25] Therefore, it is not unexpected that the 300 nm Ti_2AlN thin film was fully oxidized at 900 ºC in this work. Thermal expansion coefficients (TEC) of the oxide scale, the Ti_2AlN film and the substrates are also critical. TECs of Ti_2AlN ($\alpha_a = (8.6 \pm 0.2) \times 10^{-6}$ K^{-1}, $\alpha_c = (7.0 \pm 0.5) \times 10^{-6}$ K^{-1}, 297 - 1573 K)[24] are close with those of rutile TiO_2 ($\alpha_a = 9.2 \times 10^{-6}$ K^{-1}, $\alpha_c = 7.1 \times 10^{-6}$ K^{-1}),[24] α-Al_2O_3 ($\alpha_a = 7.9 \times 10^{-6}$ K^{-1}, $\alpha_c = 8.8 \times 10^{-6}$ K^{-1}),[24] $MgAl_2O_4$ ($8.1 \sim 9.05 \times 10^{-6}$ K^{-1})[46] and $MgTi_2O_5$ ($\alpha_a = 2.3 \times 10^{-6}$ K^{-1}, $\alpha_b = 8.1 \times 10^{-6}$ K^{-1} and $\alpha_c = 13.2 \times 10^{-6}$ K^{-1})[47]. But they have larger mismatch with those of Al_2TiO_5 ($\alpha_a = 10.9 \times 10^{-6}$ K^{-1}, $\alpha_b = 20.5 \times 10^{-6}$ K^{-1}, $\alpha_c = -2.7 \times 10^{-6}$ K^{-1}, 0 - 1273 K)[24]. Large stress will be generated if Al_2TiO_5 is formed on Ti_2AlN, which may lead to crack or even spallation of the oxide scale. Likewise, large mismatch in TECs of Ti_2AlN and the substrates will also lead to coating failure upon thermal cycling. Hence, Al concentration, film thickness and thermal expansion coefficients need be carefully considered when applying Ti_2AlN thin film as oxidation resistant coatings.

IV. Conclusion

In summary, the oxidation resistance of 300 nm single crystalline Ti_2AlN thin films has been investigated by XRD, XPS, AFM and mass spectrometry. XRD results showed that bulk of the 300 nm single crystalline Ti_2AlN thin films remains structurally stable up to 700 ºC. A close look at the surface by XPS revealed that Ti_2AlN started to be oxidized at room temperature by forming TiO_2, TiN_xO_y and Al_2O_3 with surface enrichment of Al. At 500 ºC, Al atoms in the subsurface have preferentially segregated horizontally to the edges of the terraces, oxidized and clustered into discrete Al_2O_3 domes, which do not cover the entire surface uniformly. Ti and N

atoms in the surface layer (~7.1 nm thick) were therefore exposed to air and have been completely oxidized into TiO_2, N_2O and N_2. At 700 ^oC, surface of Ti_2AlN lost its characteristic hexagonal terrace morphology by transforming into round islands as a result of high temperature oxidation. At 900 ^oC, rutile TiO_2 and Al_2O_3 reacted with MgO substrate and ambient O_2 to form spinel phase ($MgTi_2O_5$ and $MgAl_2O_4$). A higher Al percentage in Ti_2AlN thin film (as close as possible to its stoichiometric value of 25%) and a suitable film thickness would promote growth of a continuous Al_2O_3 scale, which would be beneficial for its application as high-temperature protective coatings.

- **Supporting Information**

The Rietveld phase analysis of the diffraction pattern of Ti_2AlN thin film after oxidation at 900 ^oC by TOPAS software. This material is available free of charge via the Internet at http://pubs.acs.org.

- AUTHOR INFORMATION

Corresponding Authors:

*Tel.: +65-64191332

*Fax: +65-64632536

*E-mail address: jinhm@ihpc.a-star.edu.sg

**Tel.: +65-64168953

**Fax: +65-68720785

**E-mail address: sj-wang@imre.a-star.edu.sg

- **Acknowledgment**

This project was funded by Science and Engineering Research Council (SERC) and supported by Aerospace Program of A*STAR (Grant No: 112 155 0512). Mr. Lim Poh Chong from IMRE is

acknowledged for insightful discussion about XRD results.

- **References**

(1) Barsoum, M. W., The $M_{n+1}AX_n$ Phases: A New Class of Solids; Thermodynamically Stable Nanolaminates. *Prog. Solid State Chem.* **2000**, *28*, 201-281.
(2) Eklund, P.; Beckers, M.; Jansson, U.; Hogberg, H.; Hultman, L., The $M_{n+1}AX_n$ Phases: Materials Science and Thin-film Processing. *Thin Solid Films* **2010**, *518*, 1851-1878.
(3) Beckers, M.; Schell, N.; Martins, R. M. S.; Mucklich, A.; Moller, W.; Hultman, L., Nucleation and Growth of Ti_2AlN Thin Films Deposited by Reactive Magnetron Sputtering Onto MgO(111). *J. Appl. Phys.* **2007**, *102*, 074916.
(4) Barsoum, M. W.; Brodkin, D.; El-Raghy, T., Layered Machinable Ceramics for High Temperature Applications. *Scr. Mater.* **1997**, *36*, 535-541.
(5) Joelsson, T.; Horling, A.; Birch, J.; Hultman, L., Single-crystal Ti_2AlN Thin Films. *Appl. Phys. Lett.* **2005**, *86*, 111913.
(6) Beckers, M.; Schell, N.; Martins, R. M. S.; Mucklich, A.; Moller, W., Phase Stability of Epitaxially Grown Ti_2AlN Thin Films. *Appl. Phys. Lett.* **2006**, *89*, 074101.
(7) Beckers, M.; Schell, N.; Martins, R. M. S.; Mucklich, A.; Moller, W.; Hultman, L., Microstructure and Nonbasal-plane Growth of Epitaxial Ti_2AlN Thin Films. *J. Appl. Phys.* **2006**, *99*, 034902.
(8) Joelsson, T.; Flink, A.; Birch, J.; Hultman, L., Deposition of Single-crystal Ti_2AlN Thin Films by Reactive Magnetron Sputtering from a 2Ti : Al Compound Target. *J. Appl. Phys.* **2007**, *102*, 074918.
(9) Zhang, Z.; Nie, Y.; Shen, L.; Chai, J.; Pan, J.; Wong, L. M.; Sullivan, M. B.; Jin, H.; Wang, S. J., Charge Distribution in the Single Crystalline Ti_2AlN Thin Films Grown on MgO(111) Substrates. *J. Phys. Chem. C* **2013**, *117*, 11656-11662.
(10) Zhang, T.; Myoung, H. B.; Shin, D. W.; Kim, K. H., Syntheses and Properties of Ti_2AlN MAX-phase Films. *J. Ceram. Process. Res.* **2012**, *13*, S149-S153.
(11) Zhang, Z.; Jin, H.; Chai, J.; Pan, J.; Seng, H. L.; Goh, G. T. W.; Wong, L. M.; Sullivan, M. B.; Wang, S. J., Temperature-dependent microstructural evolution of Ti_2AlN thin films deposited by reactive magnetron sputtering. *Appl. Surf. Sci.* **2016**, *368*, 88-96.
(12) Garkas, W.; Leyens, C.; Renteria, A. F., Synthesis and Characterization of Ti_2AlC and Ti_2AlN MAX Phase Coatings Manufactured in an Industrial-size Coater. *Advanced Materials Research* **2010**, *89-91*, 208-213.
(13) Yang, Y.; Keunecke, M.; Stein, C.; Gao, L.-J.; Gong, J.; Jiang, X.; Bewilogua, K.; Sun, C., Formation of Ti_2AlN Phase After Post-Heat Treatment of Ti–Al–N films Deposited by Pulsed Magnetron Sputtering. *Surf. Coat. Technol.* **2012**, *206*, 2661-2666.
(14) Dolique, V.; Jaouen, M.; Cabioc'h, T.; Pailloux, F.; Guérin, P.; Pélosin, V., Formation of (Ti,Al)N / Ti_2AlN Multilayers After Annealing of TiN / TiAl(N) Multilayers Deposited by Ion Beam Sputtering. *J. Appl. Phys.* **2008**, *103*, 083527.
(15) Cabioch, T.; Alkazaz, M.; Beaufort, M.-F.; Nicolai, J.; Eyidi, D.; Eklund, P., Ti_2AlN Thin Films Synthesized by Annealing of (Ti+Al)/AlN Multilayers. *Mater. Res. Bull.* **2016**, *80*, 58-63.

(16) Low, I. M.; Pang, W. K.; Kennedy, S. J.; Smith, R. I., Study of High-Temperature Thermal Stability of MAX Phases in Vacuum. In *Strategic Materials and Computational Design:Ceramic Engineering and Science Proceedings*, Kriven, W. M.; Zhou, Y.; Radovic, M., Eds. Wiley: Hoboken, N.J., 2010; Vol. 31, pp 171-180.
(17) Pang, W. K.; Low, I. M.; Kennedy, S. J.; Smith, R. I., *In situ* Diffraction Study on Decomposition of Ti_2AlN at 1500-1800ºC in Vacuum. *Mater. Sci. Eng., A* **2010**, *528*, 137-142.
(18) Low, I. M.; Pang, W. K.; Kennedy, S. J.; Smith, R. I., High-temperature Thermal Stability of Ti_2AlN and Ti_4AlN_3: A Comparative Diffraction Study. *J. Eur. Ceram. Soc.* **2011**, *31*, 159-166.
(19) Low, I. M.; Pang, W. K., A Comparative Study of Decomposition Kinetics in MAX Phases at Elevated Temperature. In *Advanced Ceramic Coatings and Materials for Extreme Environments II*, Zhu, D.; Lin, H.-T.; Zhou, Y.; Hwang, T.; Halbig, M.; Mathur, S., Eds. John Wiley & Sons, Inc.: Hoboken, NJ, USA, 2013; pp 179-185.
(20) Zhang, Z.; Jin, H.; Chai, J.; Shen, L.; Seng, H. L.; Pan, J.; Wong, L. M.; Sullivan, M. B.; Wang, S. J., Desorption of Al and Phase Transformation of Ti_2AlN MAX Thin Film upon Annealing in Ultra-High-Vacuum. *J. Phys. Chem. C* **2014**, *118*, 20927-20939.
(21) Barsoum, M. W., Oxidation of $Ti_{n+1}AlX_n$ (n=1-3 and X = C, N) - I. Model. *J. Electrochem. Soc.* **2001**, *148*, C544-C550.
(22) Barsoum, M. W.; Tzenov, N.; Procopio, A.; El-Raghy, T.; Ali, M., Oxidation of $Ti_{n+1}AlX_n$ (n=1-3 and X = C, N) - II. Experimental Results. *J. Electrochem. Soc.* **2001**, *148*, C551-C562.
(23) Tallman, D. J.; Anasori, B.; Barsoum, M. W., A Critical Review of the Oxidation of Ti_2AlC, Ti_3AlC_2 and Cr_2AlC in Air. *Materials Research Letters* **2013**, *1*, 115-125.
(24) Cui, B.; Sa, R.; Jayaseelan, D. D.; Inam, F.; Reece, M. J.; Lee, W. E., Microstructural Evolution During High-temperature Oxidation of Spark Plasma Sintered Ti_2AlN Ceramics. *Acta Mater.* **2012**, *60*, 1079-1092.
(25) Wang, Q. M.; Garkas, W.; Flores Renteria, A.; Leyens, C.; Sun, C.; Kim, K. H., Oxidation Behaviour of a Ti_2AlN MAX-phase Coating. *IOP Conference Series: Materials Science and Engineering* **2011**, *18*, 082025.
(26) Wang, Q. M.; Garkas, W.; Renteria, A. F.; Leyens, C.; Kim, K. H., Oxidation Behaviour of Ti_2AlN Films Composed Mainly of Nanolaminated MAX Phase. *J. Nanosci. Nanotechnol.* **2011**, *11*, 8959-8966.
(27) Graciani, J.; Sanz, J. F.; Asaki, T.; Nakamura, K.; Rodriguez, J. A., Interaction of Oxygen with TiN(001): N $\leftrightarrow$ O Exchange and Oxidation Process. *J. Chem. Phys.* **2007**, *126*, 244713.
(28) Wang, X. H.; Zhou, Y. C., High-temperature Oxidation Behavior of Ti_2AlC in Air. *Oxid. Met.* **2003**, *59*, 303-320.
(29) Wang, X. H.; Zhou, Y. C., Oxidation Behavior of Ti_3AlC_2 at 1000-1400 ºC in Air. *Corros. Sci.* **2003**, *45*, 891-907.
(30) Esaka, F.; Furuya, K.; Shimada, H.; Imamura, M.; Matsubayashi, N.; Sato, H.; Nishijima, A.; Kawana, A.; Ichimura, H.; Kikuchi, T., Comparison of surface oxidation of titanium nitride and chromium nitride films studied by x-ray absorption and photoelectron spectroscopy. *J. Vac. Sci. Technol.,A* **1997**, *15*, 2521-2528.
(31) Milošv, I.; Strehblow, H. H.; Navinšek, B.; Metikoš-Huković, M., Electrochemical and Thermal Oxidation of TiN Coatings Studied by XPS. *Surf. Interface Anal.* **1995**, *23*, 529-539.
(32) Moulder, J. F.; Stickle, W. F.; Sobol, P. E.; Bomben, K. D., *Handbook of X-ray Photoelectron Spectroscopy: A Reference Book of Standard Spectra for Identification and Interpretation of XPS Data*; Physical Electronics, Inc.: 6509 Flying Cloud Drive, Eden Prairie, Minnesota 55344, United States of America, 1995.

(33) Powell, C. J.; Jablonski, A., *NIST Electron Inelastic-Mean-Free-Path Database - Version 1.2*; National Institute of Standards and Technology: Gaithersburg, MD, USA, 2010.
(34) Mattogno, G.; Righini, G.; Montesperelli, G.; Traversa, E., XPS Analysis of the Interface of Ceramic Thin Films for Humidity Sensors. *Appl. Surf. Sci.* **1993**, *70*, 363-366.
(35) Das, S., The Al-O-Ti (Aluminum-Oxygen-Titanium) System. *J. Phase Equilib.* **2002**, *23*, 525-536.
(36) Emmerlich, J.; Hogberg, H.; Sasvari, S.; Persson, P. O. A.; Hultman, L.; Palmquist, J. P.; Jansson, U.; Molina-Aldareguia, J. M.; Czigany, Z., Growth of Ti_3SiC_2 Thin Films by Elemental Target Magnetron Sputtering. *J. Appl. Phys.* **2004**, *96*, 4817-4826.
(37) Buchholt, K.; Eklund, P.; Jensen, J.; Lu, J.; Spetz, A. L.; Hultman, L., Step-flow Growth of Nanolaminate Ti_3SiC_2 Epitaxial Layers on 4H-SiC(0001). *Scr. Mater.* **2011**, *64*, 1141-1144.
(38) Buchholt, K.; Eklund, P.; Jensen, J.; Lu, J.; Ghandi, R.; Domeij, M.; Zetterling, C. M.; Behan, G.; Zhang, H.; Lloyd Spetz, A.; Hultman, L., Growth and Characterization of Epitaxial Ti_3GeC_2 Thin Films on 4H-SiC(0001). *J. Cryst. Growth* **2012**, *343*, 133-137.
(39) Jin, H.; Zhang, Z.; Nie, Y.; Zeng, Y.; Shen, L.; Sullivan, M. B.; Wang, S. J., Interfacial Structure of Ti_2AlN Thin Films on MgO(111). *J. Phys. Chem. C* **2013**, *117*, 16515-16522.
(40) Zhang, Z.; Jin, H.; Pan, J.; Chai, J.; Wong, L. M.; Sullivan, M. B.; Wang, S. J., Origin of Al Deficient Ti_2AlN and Pathways of Vacancy-Assisted Diffusion. *J. Phys. Chem. C* **2015**, *119*, 16606-16613.
(41) Frodelius, J.; Lu, J.; Jensen, J.; Paul, D.; Hultman, L.; Eklund, P., Phase Stability and Initial Low-Temperature Oxidation Mechanism Of Ti_2AlC Thin Films. *J. Eur. Ceram. Soc.* **2013**, *33*, 375-382.
(42) Milosev, I.; Strehblow, H. H.; Navinsek, B., Comparison of TiN, ZrN and CrN hard nitride coatings: Electrochemical and thermal oxidation. *Thin Solid Films* **1997**, *303*, 246-254.
(43) Pang, W. K.; Low, I. M.; O'Connor, B. H.; Peterson, V. K.; Studer, A. J.; Palmquist, J. P., In situ Diffraction Study of Thermal Decomposition in Maxthal Ti_2AlC. *J. Alloys Compd.* **2011**, *509*, 172-176.
(44) Kerr, J. A., *CRC Handbook of Chemistry and Physics*, 81st ed.; CRC Press: Boca Raton, Florida, USA, 2000.
(45) Panjan, P.; Navinšek, B.; Čekada, M.; Zalar, A., Oxidation Behaviour of TiAlN Coatings Sputtered at Low Temperature. *Vacuum* **1999**, *53*, 127-131.
(46) Kapralik, I., Thermal Expansion of Spinels $MgCr_2O_4$, $MgAl_2O_4$ and $MgFe_2O_4$. *Chemicke Zvesti* **1969**, *23*, 665-670.
(47) Giordano, L.; Viviani, M.; Bottino, C.; Buscaglia, M. T.; Buscaglia, V.; Nanni, P., Microstructure and Thermal Expansion of Al_2TiO_5-$MgTi_2O_5$ Solid Solutions Obtained by Reaction Sintering. *J. Eur. Ceram. Soc.* **2002**, *22*, 1811-1822.

Table of Contents (TOC) Image